3-1-2022

High definition tDCS effect on postural control in healthy individuals: Entropy analysis of a crossover clinical trial

Diandra B. Favoretto

Eduardo Bergonzoni

Diego Carvalho Nascimento

Francisco Louzada

Tenysson W. Lemos

See next page for additional authors

10.3390/app12052703

Favoretto, D. B., Bergonzoni, E., Nascimento, D. C., Louzada, F., Lemos, T. W., Batistela, R. A., ... & Edwards, T. G. (2022). High definition tDCS effect on postural control in healthy individuals: entropy analysis of a crossover clinical trial. Applied Sciences, 12(5), 2703. https://doi.org/10.3390/app12052703

applied sciences

MDPI

Article

High Definition tDCS Effect on Postural Control in Healthy Individuals: Entropy Analysis of a Crossover Clinical Trial

Diandra B. Favoretto [1,*], Eduardo Bergonzoni [1], Diego Carvalho Nascimento [2,*], Francisco Louzada [3], Tenysson W. Lemos [4], Rosangela A. Batistela [4], Renato Moraes [4], João P. Leite [1], Brunna P. Rimoli [1], Dylan J. Edwards [5,6] and Taiza G. S. Edwards [1]

1 Department of Neuroscience and Behavior Sciences, Ribeirao Preto Medical School, University of Sao Paulo, Ribeirao Preto 14015-010, Brazil; dubergonzoni@usp.br (E.B.); jpleite@fmrp.usp.br (J.P.L.); brunna.rimoli@usp.br (B.P.R.); taiza@fmrp.usp.br (T.G.S.E.)
2 Departamento de Matemática, Facultad de Ingeniería, Universidad de Atacama, Copiapó 1530000, Chile
3 Institute of Mathematical Science and Computing, University of Sao Paulo, Sao Carlos 13566-590, Brazil; louzada@icmc.usp.br
4 School of Physical Education and Sport of Ribeirao Preto, University of Sao Paulo, Ribeirao Preto 14040-907, Brazil; tenysson@fmrp.usp.br (T.W.L.); rosangela_batistela@usp.br (R.A.B.); renatomoraes@usp.br (R.M.)
5 Moss Rehabilitation Research Institute, Elkins Park, PA 19027, USA; EdwardDy@einstein.edu
6 Exercise Medicine Research Institute, Edith Cowan University, Joondalup 6027, Australia
* Correspondence: diandrafavoretto@usp.br (D.B.F.); diego.nascimento@uda.cl (D.C.N.)

Abstract: Objective: Converging evidence supporting an effect of transcranial direct current stimulation (tDCS) on postural control and human verticality perception highlights this strategy as promising for post-stroke rehabilitation. We have previously demonstrated polarity-dependent effects of high-definition tDCS (HD-tDCS) on weight-bearing asymmetry. However, there is no investigation regarding the time-course of effects on postural control induced by HD-tDCS protocols. Thus, we performed a nonlinear time series analysis focusing on the entropy of the ground reaction force as a secondary investigation of our randomized, double-blind, placebo-controlled, crossover clinical trial. Materials and Methods: Twenty healthy right-handed young adults received the following conditions (random order, separate days); anode center HD-tDCS, cathode center HD-tDCS or sham HD-tDCS at 1, 2, and 3 mA over the right temporo-parietal junction (TPJ). Using summarized time series of transfer entropy, we evaluated the exchanging information (causal direction) between both force plates and compared the dose-response across the healthy subjects with a Generalized Linear Hierarchical/Mixed Model (GLMM). Results: We found significant variation during the dynamic information flow ($p < 0.001$) among the dominant bodyside (and across time). A greater force transfer entropy was observed from the right to the left side during the cathode-center HD-tDCS up to 2 mA, with a causal relationship in the information flow (equilibrium force transfer) from right to left that decreased over time. Conclusions: HD-tDCS intervention induced a dynamic influence over time on postural control entropy. Right hemisphere TPJ stimulation using cathode-center HD-tDCS can induce an asymmetry of body weight distribution towards the ipsilateral side of stimulation. These results support the clinical potential of HD-tDCS for post-stroke rehabilitation.

Keywords: high-definition transcranial direct current stimulation; postural control; entropy; nonlinear time series

Citation: Favoretto, D.B.; Bergonzoni, E.; Nascimento, D.C.; Louzada, F.; Lemos, T.W.; Batistela, R.A.; Moraes, R.; Leite, J.P.; Rimoli, B.P.; Edwards, D.J.; Edwards, T.G.S. High Definition tDCS Effect on Postural Control in Healthy Individuals: Entropy Analysis of a Crossover Clinical Trial. *Appl. Sci.* **2022**, *12*, 2703. https://doi.org/10.3390/app12052703

Academic Editor: Pentti Nieminen

Received: 31 December 2021
Accepted: 28 February 2022
Published: 5 March 2022

1. Introduction

Stroke is a cerebrovascular disease, and is the second major cause of death and disability worldwide [1]. About 30–50% of patients become dependent when it comes to activities of daily living (ADL) [2]. The postural imbalance leads to functional deficits and may occur due to changes in mechanical components such as muscle weakness, limitation of joint movement, changes in muscle tone, as well as sensory damage and neuromuscular

synergies [3]. The visual verticality perception (VV) disorder, the incapacity to judge the orientation of the body or environment in relation to Earth vertical within normal limits, is commonly observed after stroke and is associated with poor balance [4]. When in a standing position, patients with VV disorder present a weight asymmetry towards the opposite side of the VV tilt as a compensatory strategy to maintain their center of gravity within the limits of stability [5–8].

Lesions of the temporo-parietal junction (TPJ), a hub area for multisensory integration, can cause VV disorder and postural imbalance [9]. Non-invasive brain stimulation (NIBS) techniques, such as conventional and high-definition transcranial direct current stimulation (HD-tDCS) are current therapeutic resources with potential modulation over the pathophysiology and behavior of brain mechanisms [10]. Recently, we have observed significant effects of conventional non-invasive transcranial stimulation (tDCS) [11] and HD-tDCS [12] applied over the TPJ in both healthy subjects and patients after stroke.

Clinical VV and weight-bearing asymmetry (WBA) disorders described in patients after stroke [4,12,13] were reproduced in healthy individuals after using our stimulation protocol. We found the effect was dependent on the cathode center condition with induction of WBA towards the side of brain stimulation [12] with no dependency on the electrical current intensity. Other studies evaluated electroencephalography (EEG) after our HD-tDCS protocol in healthy subjects and suggested entropy (nonlinear outcome) of EEG as a robust alternative for temporal data analysis complementing linear analysis [14].

We hypothesized that the HD-tDCS would induce a sequence of events on postural control demonstrated by an influence in the WBA. Thus, we analyzed the ground reaction force in each platform through the flow of information using transfer entropy. This type of entropy was selected given the possibility of a causal interpretation, as well as the ability to reduce the problematic complexity by incorporating time dependence with simplicity [15].

2. The Data

This study was conducted using experimental data collected according to the Helsinki Declaration requirements for human investigation and was approved by the local ethics committee. All twenty participants provided written informed consent. This article followed the guidelines of the Checklist of Information to include when reporting a randomized trial following the Consolidated Standards of Reporting Trials (CONSORT) for randomized trials.

2.1. Participants

The study included a distinct sample population blinded to the HD-tDCS approach for assessing ground reaction force. The study candidates were healthy subjects aged between 20 to 28 years, male and female, right-handed, non-smokers, with no evidence of brain, vestibular or orthopedic dysfunction, with normal or corrected vision. To ensure the absence of vestibular deficits, oculomotor tests, the head shake, and head thrust, tests were accomplished. The assessment period was 10 months.

2.2. Intervention

We used the HD-tDCS protocol organized in the 3 × 1 standard. The assembly was composed of a central electrode on the right cerebral hemisphere TPJ and three peripheral electrodes located at EEG coordinates P4, C4, and T8. We used a Soterix HD-tDCS device (Soterix Medical®, New York, NY, USA). During and after the application of the electric current, we assessed the body movement kinetics measured by two force plates (Bertec 4060-NC, Columbus, OH, USA) in the static orthostatic posture of each individual, verified by the WBA (Figure 1).

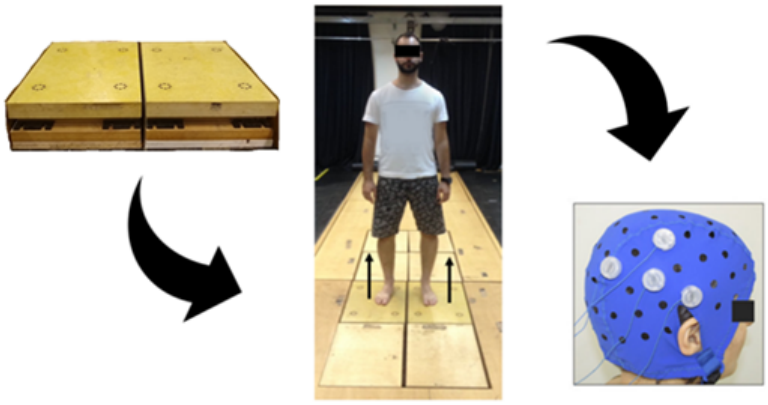

Figure 1. Illustration of the WBA study protocol. The left-hand side figure exhibits the platforms. In the middle, an illustration of a participant positioned on this equipment. The right-hand side shows the position of the high definition transcranial stimulation (HD-tDCS) electrodes.

2.3. Outcome Measure

Each volunteer underwent three different randomized HD-tDCS conditions (cathode-central, anode-central, and sham) on three different days. Each HD-tDCS condition was applied in a sequence of three stimulation intensities (1, 2, and 3 mA) repeated three times. Each stimulation intensity was conducted for 2 min with a rest interval of 5 min. The intervention performed on this study followed the stimulation protocol previously validated and published by our group [12]. Detailed analysis of the stimulation protocol, as well as dose calculation for each stimulation session, HD-tDCS computational modeling, induced current flow, safety and tolerability criteria, randomization protocol, and allocation concealment of this study were published elsewhere [12].

The experiment consisted of ten blocks of tasks (baseline and three replicas of each condition), and data were collected during and after each one (online and offline). For each condition (cathode-central, anode-central, and sham), we acquired the vertical force component (Fz), after baseline and each stimulation period, in real-time for the two platforms (Right-side and Left-), with a resolution of 100 Hz, for 2 min. That returns a time series Fz of 24,000 records (12,000 online and 12,000 offline) per block, for each platform. The full protocol resulted in 28,800,000 observations, given that we observed 20 subjects and each one of them holds three trials, returning a total of 30 blocks of tasks per participant. That is, a single individual had 1,440,000 observations (720,000 observations per platform). Later, we quantified the Fz component information flux across the platforms (Right-side $\rightarrow$ Left-, and Left-side $\rightarrow$ Right-) using the transfer entropy (TE). Then, our final database was reduced to 2400 observations (120 records per individual, originated form the 30 tasks $\times$ 2 moments [on- & off-line] $\times$ 2 sides [$R \rightarrow L$ & $L \rightarrow R$]).

2.4. Statistical Analyses

In the statistical context, entropy measures complexity between signal data or time series (TS) that links the amount of information to a probability distribution [16,17]. One option for analyzing and modeling the entire TS is to apply summary statistics, for example, the processor average.

We have previously outlined a dose-response model testing the intensity and polarity-dependent effect of HD-tDCS, and compared the effect of anodal and cathodal stimulation polarity at different intensities (1 mA, 2 mA, and 3 mA) in VV, electroencephalogram (EEG), and WBA [12]. Furthermore, an entropy-based study was performed and discussed following the same protocol using only the EEG results in a deeper discussion, whereas significant statistical results comparing Cathodal vs. Anodal montage in the intensity of 2 mA was noticeable [14]. Nonetheless, a discussion about the different responses across

the Sham-Cathodal and Sham-Anodal continues to be a gap when it comes to tDCS clinical studies [18].

We adopted the Transfer Entropy (TE) in the data, which considers a measurement of directional information transfer among two random processes, and it is always positive. For instance, considering two random processes, $W1_t$ and $W2_t$, indexed in the time $t \in N$. Through the Shannon entropy, H(.), and considering L the length of an embedded vector or history length (underlying state of the Markov process, further information, please see [19]), the TE is calculated as:

$$TE_{W1 \to W2} = H(W2_t | W2_{t-1:t-L}) - H(W2_t | W2_{t-1:t-L}, W1_{t-1:t-L}). \quad (1)$$

The time series process was analyzed using entropy index for all data acquired towards the complexity of the Fz component of the platforms after baseline or the stimulation protocol application, as shown in the data pre-processing procedure in Figure 2.

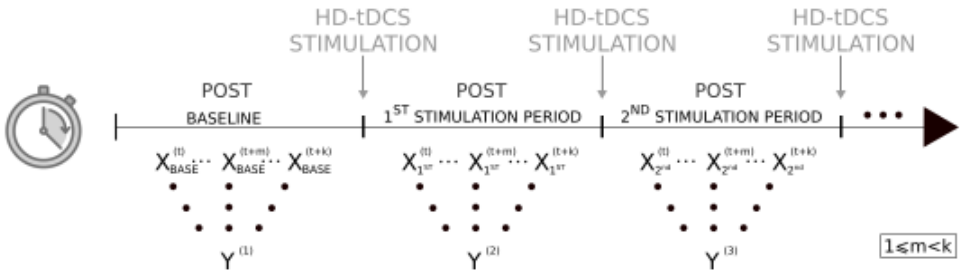

Figure 2. Visual representation of the data transformation method in which fixing a time window t, the impact of one time series into the other, represented by ($X^{(t)}$), is summarized into entropy index ($Y^{(t)}$). For each experiment period, the transfer entropy calculation was done per segmentation (time window), which transformed the exchanged information (causal direction) between one platform into a complexity measure value (entropy index). The entropy index calculated the causal effect from the right-side to the left-side of a time segment, as well the effect of the same time segment from the left-side to the right.

We evaluated the effect of HD-tDCS applied in the TPJ on postural control, observing the intensity for each combination of condition and intensity. Thus, using the transfer entropy [15,20] as an entropy measure has enabled to encompass whether the past state of one Fz signal could improve the prediction of the other Fz signal on each platform (right-side to the left, and vice-versa), addressing the causal inference among the Fz components. Moreover, with the transfer entropy, one measures the causal direction and enables to test such statement, and if existent, one can compare whether a dominant side impacts the other or reverse.

Therefore, we sought to compare the TS causality summarized across the different moments, using Mixed-Effect Models (considering random intercept for each individual that can present a personal characteristic). Furthermore, as a Longitudinal study (in which the same individual is observed multiple times and on different days), to distinguish between stimulus types versus intensity and to quantify the differences in regularity between the platforms.

As the hypotheses were defined in advance, we used a global test between comparison treatments complexity. A significance level of 5% was considered in all tests. Statistical analyses were performed using R software for Statistical Computing and Analysis. The descriptive results of the figures were presented as the difference from the baseline. We described Transfer Entropy (TE) and Generalized Linear Mixed-Effect Models (GLMM).

This study adopted the implemented TE function from the *RTransferEntropy* package, and the implemented GLMM from the *lme4* and *lmerTest* packages to test the linear contrasts of fixed effects (estimate the p-values), all in R software [21].

Additionally, the Kruskal–Wallis test was adopted in order to check the statistical significance between Sham-Anodal versus Sham-Cathodal stimulation, to test the difference, in each time period, across their information flux between the force places (that is, observing the Left→Right, and also the Right→Left), further information [22,23]. Moreover, given the open gap in the literature on the different biological effects concerning the sham condition [18], in this study we highlighted this comparison in each time period block. Furthermore, the discussion on these findings is related to the existence of a carryover effect between pre/post stimulation versus baseline [24].

For better understanding, Figure 3 visually represents the present methodology framework, from importing data to extracting its information.

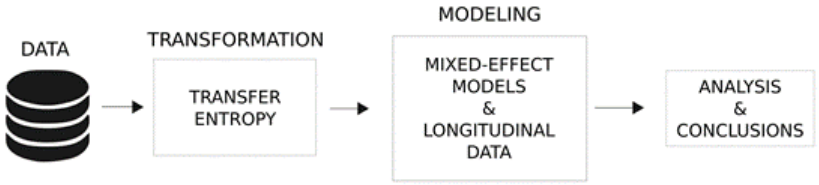

Figure 3. Visual summary of the methodological framework. Acquired data transformation was obtained by using the bi-dimensional time series related to the vertical platform (Fz) from the right and left side, then summarizing each piece of transference information as a complexity measure (using the transfer entropy). After summarizing these data into single values, they were compared using a Mixed-Effect Model (GLMM, Gamma Regression), as a longitudinal study. Then, analysis and conclusions were drawn.

3. Results

A total of 20 consecutive healthy subjects were included in the study, in mean age of 24.2 ± 4.1 years. There were 13 women and eight men, all right-handed. All volunteers accomplished the three days of HD-tDCS stimulation protocol with posturography evaluations.

In the literature, it is often common to find only discussions towards functional connectivity. This limits inferences to the ones related to the statistical covariation of signals, typically revealed by cross-correlograms or coherence measures. Therefore, effective connectivity is more suitable for explaining causal relationships, that is, the time dependence across the platform signals.

As for the HD-tDCS dose-response analysis of WBA, we found a decrease in entropy on each platform (with suggestion to add determinism in the system, creating a pattern among the post-stimulation period), as shown in Figure 4C. Moreover, visually, there is an increase in the variability (across the montages) on 2 mA (Figure 4B), as well as a causal effect from the right side on the left (Figure 4A).

The robustness in the dominant side (causal effect from the right-side to the left-) is also observed (Figure 4B), in which the right-hand panel presents shorter transfer entropy variation on the dose-response.

Considering a possible accumulated effect of the stimulation over our behavioral measure [25], we observed the mean response of the entropy for the baseline and each pre/post-stimulation condition to analyze the carryover effect of our HD-tDCS protocol. Visually, we show a similar mean response independent of the conditions (baseline, Anodal (AC), Sham-AC, Cathodal (CC), Sham-CC) and the side of the platform (Figure 5), which suggests that our 5 min interval between each HD-tDCS stimulation was enough to avoid a carryover effect over the entropy.

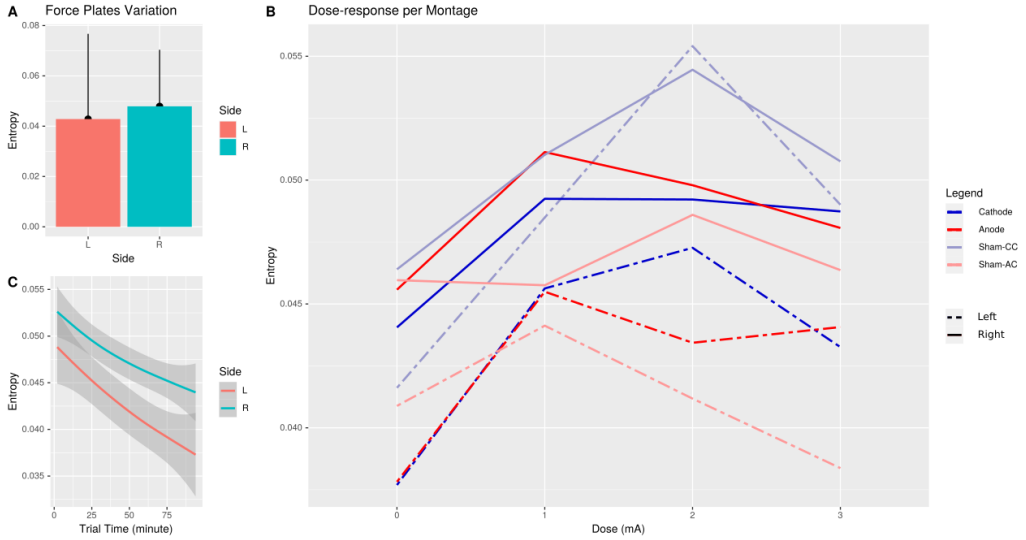

Figure 4. Comparison across the Fz measurements from the platforms and dose-response on each montage. Panel **A** represents the mean causal entropy from the left side to the right (L) and from the right side to the left (R). The black lines represent one standard error. Panel **B** shows the transfer entropy of each platform per montage across the dose-response, time-invariant. Panel **C** displays the nonlinear dynamic and complexity of each platform across time, smoothing the entropy trials evolution through a generalized additive model (GAM) and considering a confidence interval of 95%.

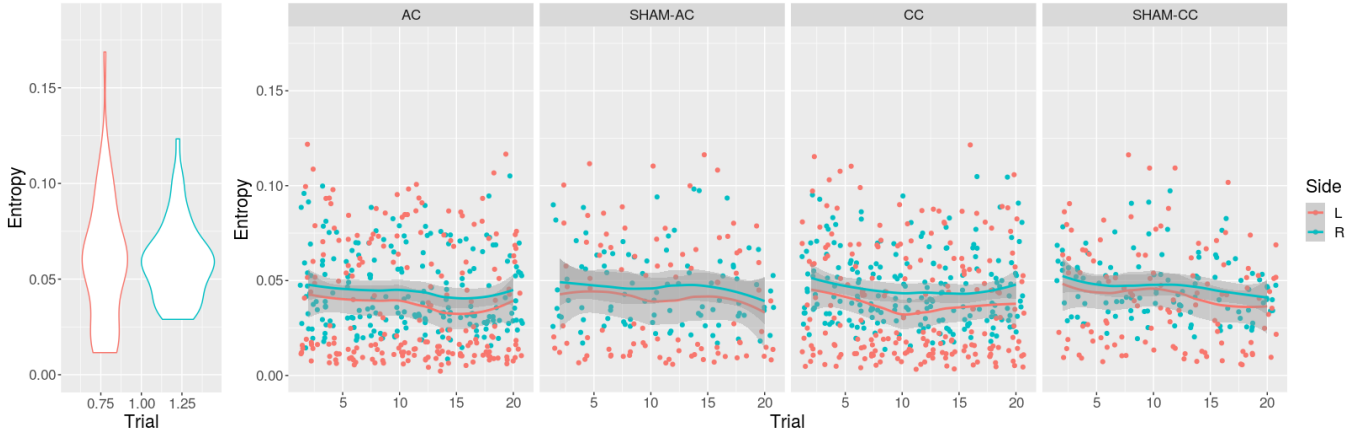

Figure 5. The left-hand plot shows the baseline entropy. The other plots show the time-varying pre/post stimulation entropy responses (off-line) across different montages, per side. The visualization adopted the LOESS smoothness, which shows that all montage presents equivalent mean entropy response regardless of its side (Left → Right represented by L, and Right → Left by R), therefore, showing no carryover effect.

In order to keep the participants blinded to the interventions [18], we used a sham protocol, as described in details elsewhere [12]. In a few words, the sham condition consisted of nine repetitions per block, starting with a Ramp-Up of 30 s for each current intensity block (1 mA, 2 mA e 3 mA), immediately followed by a Ramp-Down of 30 s and 2 min with no current intensity (0 mA), in which our outcome variable (Fz component of each platform) was acquired, then transformed into TE complex measure. The first point to be analyzed consisted of comparing the Sham-Anodal versus Sham-Cathodal across replicas within distinct trials phases (whereas their descriptions are presented in Table 1).

Table 1. Descriptive comparison between Sham-Anodal and Sham-Cathodal.

	Stimuli Moment	Sham-Anodal Median [Range]	Sham-Cathodal Median [Range]
Right → Left	PRE or POST (OFF)	0.0397 [0.02, 0.10]	0.0438 [0.02, 0.10]
	1 mA (ON)	0.0314 [0.01, 0.10]	0.0429 [0.01, 0.13]
	2 mA (ON)	0.0433 [0.02, 0.12]	0.052 [0.01, 0.10]
	3 mA (ON)	0.0373 [0.02, 0.10]	0.0481 [0.01, 0.09]
Left → Right	PRE or POST (OFF)	0.0266 [0.01, 0.12]	0.0396 [0.01, 0.12]
	1 mA (ON)	0.0225 [0.01, 0.13]	0.0393 [0.00, 0.16]
	2 mA (ON)	0.0205 [0.01, 0.15]	0.0667 [0.01, 0.13]
	3 mA (ON)	0.0206 [0.01, 0.11]	0.0469 [0.00, 0.11]

Table 2 shows the Kruskal–Wallis tests' p-values across the Sham montages comparison (Anodal, AC, versus Cathodal, CC), for each TE response, within stimuli off (pre/post-stimulation) or during stimuli (1, 2, or 3 mA), in which none of them presented statistically different patterns within the observed group (limited to the sample size observed in this protocol study). It is noteworthy that Sham-AC shows an equivalent pattern to the Sham-CC.

Table 2. Kruskal–Wallis tests considering each force place (information flux comes from the Left-side, Left → Right, or Right-side, Right → Left) across the difference between Sham-Anodal versus Sham-Cathodal stimulation observation per period.

	***p*-Value**	
Stimuli Moment	**Left-Side**	**Right-Side**
PRE or POST (OFF)	0.529	0.505
1 mA (ON)	0.791	0.375
2 mA (ON)	0.099	0.214
3 mA (ON)	0.255	0.408

A theoretical GLMM was adopted to explain the Transfer Entropy dynamic through a combination of montages and intensity, the variables time and platform side (if the transfer information is from the Right-side or the Left-side to the other), and also considering that each participant shows a personal response (that is, as a latent effect). Moreover, this regression structure is explained with multiplicative error, then as a GLMM with Gamma distribution considering a logarithmic link, and the stochastic component is described by a Gamma model with scale parameter ν, observation of k participants in groups i -Montages- and j -Doses-, for $k = \{1, \ldots, 20\}$, $i = \{$"Baseline", "Sham-Cathodal", "Sham-Anodal", "Cathodal", "Anodal"$\}$ and $j = \{$"0 mA (Pre- or Post-Stimulation)", "1 mA", "2 mA", "3 mA"$\}$. That is,

$$\text{Transfer entropy response } (Y_{ijk}) \sim Gamma(y_{ijk}\mu_{ijk}, \nu) \quad (2)$$

$$\mu_{ijk} := \mathbb{E}[Y_{ij}\boldsymbol{X_{ij}}] = e^{\boldsymbol{X_{ij}\beta}+Z_{ijk}\gamma_k} \quad (3)$$

$$\text{whereas } \boldsymbol{X_{ij}\beta} = \beta_1^{(i)} Montage + \beta_2^{(j)} Dose + \beta_3^{(ij)} Montage * Dose + \beta_4 Time + \quad (4)$$

$$\beta_5 Side + \beta_6 Time * Side \quad (5)$$

in which $\boldsymbol{X_{ij}}$ is the described array of known fixed effects explanatory variables, β is the p-dimensional vector of fixed effects coefficients, Z_{ijk} is the array of known personal random effects explanatory variables and γ_k is the q-dimensional vector of personal random effects (normally distributed with mean equal to zero).

The GLMM brings the results related to montage, intensity, time, and side (complete table in Appendix A, and its Bayesian version, which also contains the effective sample size estimate in Appendix B). Fixing each intensity and observing the interaction among

montages, cathodal condition up to 2 mA presented statistically different against Sham (Figure 6). The decrease in the entropy on the left platform was influenced by the flow of information from the right side. Furthermore, the time of the stimulation (duration and repetition) appeared to be an influential factor in the changes in the entropy signal.

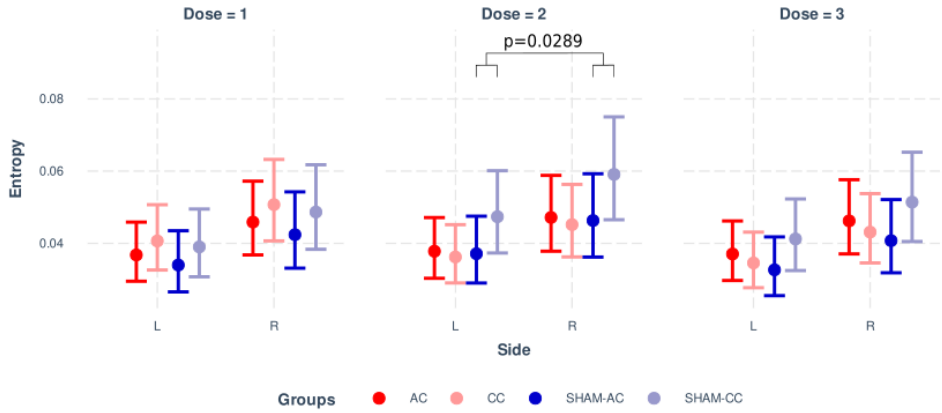

Figure 6. Comparison of the entropy measurements across the different brain stimulation conditions, and the interaction effects between categorical predictors from the adjusted GLMM [26]. The results indicate that our sham protocol would not yield effects in our variable of interest and that the cathode center condition induced a significant effect on the postural control.

4. Discussion

The transfer entropy (TE) analysis presented here contributes to the findings reported by our group that described the effects of HD-tDCS on postural control. Here we evaluated predictive information between the right and left sides of the WBA, showing a causal relationship from the right side to the left side. Moreover, we showed an effect of the intensity up to 2 mA with the cathodal condition. Therefore, empirical evidence related to the HD-tDCS on postural control over right-hemisphere TPJ is statistically noticeable, as a modulator, in healthy subjects.

Previous studies indicate that, with a disturbed bipedal stance in healthy participants [27,28], as well as in post-stroke participants [29], greater WBA is observed. The findings of Genthon and Rougier [27] showed an increase in the mediolateral amplitude of the CoP, more evident for the unloaded foot. Following similar directions but without an effect of side, L.C. Anker et al. [28] highlighted that the mediolateral velocity of the CoP had a linear increase with the WBA. Both studies suggest a decrease in postural stability with more WBA in healthy participants. In people after stroke, Marigold and Eng [30,31] reported a moderate association between WBA and large CoP velocities, whereas Manfield et al. [32] showed an association between WBA and between-limb synchronization. We have confirmed, in this study, that our HD-tDCS protocol over the right TPJ in healthy individuals is capable of replicating the behavior of post-stroke VV misperception. The cathodal 2 mA stimulation yields less weight discharge to the left leg, resulting in a loss of complexity of the force plate signal caused by a greater discharge in the right leg, i.e., flow of information (Transfer Entropy) from the right side to the left.

Several previous studies explored some of the various physiological rhythms of the human body [33–36]. Among them, we can describe the system responsible for postural control, in which the oscillations in a temporal series of postural stability establish the physiological rhythm relative to this system. Previously, postural oscillations were believed to comprise static and stationary order [37,38]. However, more recent research has proven the nonlinear characteristics of the human posture stability time series [39–42]. The discriminatory capacity of various entropy methods in the differentiation of two COP paradigms was confronted in falling and non-falling elderly. They evaluated postural control in both groups of elderly with eyes open (EO) and eyes closed (EC). The authors found

that Multiscale Entropy (MSE) and Composite Multiscale Entropy (CompMSE) presented the best ability to discriminate between falling and non-falling [43]. The structure of COP trajectories under stroke patients' paretic and non-paretic foot was examined and showed that the COP profiles under the non-paretic foot were the most regular, showing lower sample entropy [44]. When it comes to using nonlinear measures, there is some consensus in the literature showing a decrease in the complexity of the CoP signals in people with diseases [45]. This is suggested by the "loss of complexity hypothesis" pointed by Lipsitz and Goldberg, showing a less capable system to adapt to situations in order to execute tasks because of deterioration in health [46,47]. The literature confirms the entropy analysis as a promising tool to evaluate the postural control of health and individuals with specific conditions. However, none of them analyzed the causal relationships between time series in postural control.

Approximate entropy (ApEn) is a measure of system complexity initially applied to cardiovascular physiological data. It measures how similar two sequences of a specific length in the next point of a TS are. A new entropy algorithm was developed to reduce the bias of ApEn, i.e., counting self-matched sequences. Sample entropy (SampEn) does not count self-matches and has more relative consistency than ApEn [17]. Another technique, multiscale entropy (MSE), proposed to use SampEn to calculate entropy in different time scales. It can be applied to investigate physiological deficits at each time scale that can be related to postural fluctuations [48]. The aforementioned entropy families have been used to measure fluctuations in sequences of a TS but are not able to infer causality between these sequences of points or two different sources of TS. Based on Information Theory, TE is used to measure dependency between two TS and is capable to detect effective connectivity based on interaction delays between the signals [15,20]. Additionally, our methodology with GLMM was able to show elements in favor, for the first time, the dynamics of the TE between the two Fz components of the platforms with a causal relationship from the right to the left side. The time (duration and repetition) of stimulation also shows an effect over the TE, showing that our specific protocol of HD-tDCS over the TPJ is able to promote changes in WBA.

Future studies are necessary to explore random effects related to personal characteristics to promote a broader knowledge involving causality on dynamic entropy data. Moreover, each person shows a particular baseline towards the central (spatial) force-displacement, and a more complex statistical structure can be accommodated, such as spatial-domain in this data-driven modeling [49].

As a natural evolution of this study, we shall explore spatial dynamic responses, which will shed light on the postural control task, and stimulation timing. This can be added in further statistical modeling and can be incorporated as latent effect information. This can be explained by the upright quiet standing postural control being an unstable condition involving the body counteracting the force of gravity. In order to keep the center of mass within the base of support, the individuals depend on somatosensory information that comes from body segments organization, muscular activity, body orientation, and vertical perception. Therefore, postural control is a complex system being affected differently by each individual and population under investigation [50].

5. Conclusions

This study supports our previous research showing that transfer entropy analyses can be used to explore the effects of dynamic time-variable parameters of stimulus (at discrete intensities) versus condition (polarity). Here we addressed the causal inference between WBA in two separate platforms in healthy subjects. We complemented the evidence of the effects elucidated by our stimulation protocol [12] with a nonlinear time-series analysis. Thus, we showed that past states of the right Fz component can improve the prediction of the left Fz component. The effects induced a WBA with a decrease in entropy over time. That is, the process, becoming more deterministic, was influenced by electrical stimulation. The visually observed greater variability of the entropy on the left side and the results of the

interaction between montage and intensity confirm that our HD-tDCS montage with the cathodal polarity and intensity of 2 mA promoted a greater effect on the postural control.

Author Contributions: D.B.F.: study concept and design of the clinical trial, data acquisition, analysis and interpretation of the clinical trial, and manuscript writing. E.B.: data acquisition, analysis and interpretation of the clinical trial, and manuscript writing. D.C.N.: statistical analysis and interpretation of data of the clinical trial, and manuscript writing. F.L.: supervision of the statistical analysis and interpretation of data of the clinical trial, and critical revision of the manuscript for intellectual content. T.W.L.: data supervision, analysis and interpretation of the clinical trial, and critical revision of the manuscript for intellectual content. R.A.B.: data acquisition, analysis and interpretation of the clinical trial, and critical revision of the manuscript for intellectual content. R.M.: data supervision and interpretation of the clinical trial, and critical revision of the manuscript for intellectual content. J.P.L.: study concept and design of the clinical trial, data supervision and interpretation, and critical revision of the manuscript for intellectual content. B.P.R.: data acquisition, analysis and interpretation of the clinical trial, and critical revision of the manuscript for intellectual content. D.J.E.: study concept and design of the clinical trial, interpretation of computational modeling, data analysis and interpretation of the clinical trial and critical revision of the manuscript for intellectual content. T.G.S.E.: study concept and design of the clinical trial, interpretation of computational modeling, data acquisition, analysis and interpretation of the clinical trial, and manuscript writing. All authors have read and agreed to the published version of the manuscript.

Funding: Diego Nascimento acknowledges the support from the São Paulo State Research Foundation (FAPESP process 2020/09174-5). Francisco Louzada acknowledges the support from the São Paulo State Research Foundation (FAPESP Processes 2013/07375-0) and CNPq (grant no. 301976/2017-1). Taiza Edwards acknowledges the support from CAPES (Finance Code 001).

Institutional Review Board Statement: The studies involving human participants were reviewed and approved by Joao P. Leite—Department of Neuroscience and Behavioral Sciences, Ribeirao Preto Medical School, University of São Paulo. The patients/participants provided their written informed consent to participate in this study.

Informed Consent Statement: Informed consent was obtained from all subjects involved in the study.

Data Availability Statement: The datasets generated for this study and scripts are available on https://github.com/ProfNascimento/WBA (accessed on 10 January 2022).

Conflicts of Interest: The authors declare no conflict of interest.

Appendix A

The Appendix Section shows the complete table holding the fixed effect estimations, and their *p*-values associated, considering the GLMM gamma regression, adopting a logarithm link function.

Table A1. Mixed model—Fixed effects estimations.

	Estimate	Std. Error	*t* Value	Pr(>|z|)	
baseline	−2.8219	0.1203	−23.46	$<2 \times 10^{-16}$	***
Anodal (AC)	−3.1613	0.1068	−29.59	$<2 \times 10^{-16}$	***
Cathodal (CC)	−3.1495	0.1068	−29.48	$<2 \times 10^{-16}$	***
SHAM-AC	−3.1958	0.1107	−28.86	$<2 \times 10^{-16}$	***
SHAM-CC	−3.0344	0.1094	−27.74	$<2 \times 10^{-16}$	***
1 mA vs. 0 mA	−0.1088	0.0649	−1.68	0.0934	.
2 mA vs. 0 mA	0.1073	0.0545	1.97	0.0490	*
3 mA vs. 0 mA	−0.0899	0.0597	−1.51	0.1321	

Table A1. *Cont.*

	Estimate	Std. Error	*t* Value	Pr(>|z|)	
Time	−0.0034	0.0006	−6.13	8.6×10^{-10}	***
Right-side vs. Left-	0.1457	0.041	3.55	0.0004	***
AC vs. SHAM-CC: 1 mA	0.1142	0.0809	1.41	0.1579	
CC vs. SHAM-CC: 1 mA	0.1813	0.0804	2.25	0.0242	*
SHAM-AC vs. SHAM-CC: 1 mA	0.02619	0.0968	0.27	0.7867	
AC vs. SHAM-CC: 2 mA	−0.0299	0.0678	−0.44	0.6592	
CC vs. SHAM-CC: 2 mA	−0.1483	0.0679	−2.18	0.0289	*
SHAM-AC vs. SHAM-CC: 2 mA	−0.158	0.0811	−1.95	0.0515	.
AC vs. SHAM-CC: 3 mA	0.0303	0.0743	0.41	0.6839	
CC vs. SHAM-CC: 3 mA	−0.0033	0.0744	−0.04	0.9646	
SHAM-AC vs. SHAM-CC: 3 mA	0.0584	0.0891	0.66	0.5124	
Right-side vs. Left-: Time	0.0017	0.0008	2.17	0.0299	*
−−−					
Signif. codes:	'***' 0.001	'**' 0.01	'*' 0.05	'.' 0.1	' ' 1

Appendix B

The Appendix Section shows the complete Bayesian version of the previous GLMM, considering the GLMM gamma regression, adopting a logarithm link function. We adopted the *brms* package [51], implemented in R [52], and used as interface to Stan [53] for full Bayesian inference. By default, the Stan inference engine uses the No-U-Turn sampler (NUTS) as an adaptive form of Hamiltonian Monte Carlo (HMC) sampling for numerical approximation. We considered draws from 4 chains, each with a number of total iterations of 15,000, considering a warmup of 5000 and a thinning rate of 10. The adopted priors was non-informative for the fixed effects (β) and random effects (γ), such as,

$$\beta \sim Normal(0, 10) \quad \text{(A1)}$$

$$\gamma \sim Cauchy(0, 2) \quad \text{(A2)}$$

Table A2 shows all estimations (fixed and random effects), *Rhat* as a metric for the chain convergence diagnostic, and also presents *Bulk ESS* and *TailESS* as the effective sample size for inference validations.

Table A2. Bayesian GLMM—Fixed & Random effects estimations.

	Estimate	Std. Error	l-95% CI	u-95% CI	Rhat	Bulk ESS	Tail ESS
baseline	−2.463	3.638	−9.658	4.671	1.001	3438	3764
Anodal (AC)	−3.157	0.115	−3.380	−2.925	1.000	2128	3039
Cathodal (CC)	−3.146	0.114	−3.368	−2.912	1.001	2138	2968
SHAM-AC	−3.189	0.118	−3.423	−2.956	1.000	2204	2932
SHAM-CC	−3.028	0.116	−3.253	−2.794	1.001	2081	3043
1 mA vs. 0 mA	0.076	4.543	−8.888	9.022	1.000	3560	3726
2 mA vs. 0 mA	0.435	4.318	−8.009	8.579	1.000	3394	3553
3 mA vs. 0 mA	−0.274	4.337	−8.635	8.395	1.000	3142	3523

Table A2. *Cont.*

	Estimate	Std. Error	l-95% CI	u-95% CI	Rhat	Bulk ESS	Tail ESS
Time	−0.003	0.001	−0.005	−0.002	1.000	4073	3580
Right-side vs. Left-	0.146	0.041	0.064	0.227	1.000	3899	3913
AC vs. baseline: 1 mA	−0.071	4.543	−9.004	8.854	1.000	3542	3663
CC vs. baseline: 1 mA	−0.004	4.542	−8.956	9.027	1.000	3562	3682
SHAM-AC vs. baseline: 1 mA	−0.157	4.543	−9.086	8.816	1.000	3555	3700
SHAM-CC vs. baseline: 1 mA	−0.185	4.540	−9.130	8.746	1.000	3545	3668
AC vs. baseline: 2 mA	−0.358	4.318	−8.493	8.080	1.000	3392	3520
CC vs. baseline: 2 mA	−0.476	4.317	−8.660	7.978	1.000	3398	3587
SHAM-AC vs. baseline: 2 mA	−0.485	4.318	−8.684	8.021	1.000	3392	3520
SHAM-CC vs. baseline: 2 mA	−0.328	4.318	−8.480	8.128	1.000	3392	3553
AC vs. baseline: 3 mA	0.214	4.337	−8.458	8.524	1.000	3147	3537
CC vs. baseline: 3 mA	0.181	4.338	−8.502	8.534	1.000	3143	3524
SHAM-AC vs. baseline: 3 mA	0.242	4.336	−8.421	8.583	1.000	3146	3460
SHAM-CC vs. baseline: 3 mA	0.183	4.337	−8.485	8.534	1.000	3146	3538
Right-side vs. Left-: Time	0.002	0.001	0.000	0.003	1.000	4098	3929
—							
shape parameter	3.460	0.097	3.274	3.653	1.000	4261	4043
—							
sd(Intercept)	0.473	0.084	0.346	0.673	1.000	3286	3929

References

1. Campbell, B.C.; De Silva, D.A.; Macleod, M.R.; Coutts, S.B.; Schwamm, L.H.; Davis, S.M.; Donnan, G.A. Ischaemic stroke. *Nat. Rev. Dis. Prim.* **2019**, *5*, 1–22. [CrossRef] [PubMed]
2. Capistrant, B.D.; Wang, Q.; Liu, S.Y.; Glymour, M.M. Stroke-associated differences in rates of activity of daily living loss emerge years before stroke onset. *J. Am. Geriatr. Soc.* **2013**, *61*, 931–938. [CrossRef] [PubMed]
3. Mizuta, N.; Hasui, N.; Nakatani, T.; Takamura, Y.; Fujii, S.; Tsutsumi, M.; Taguchi, J.; Morioka, S. Walking characteristics including mild motor paralysis and slow walking speed in post-stroke patients. *Sci. Rep.* **2020**, *10*, 1–10. [CrossRef] [PubMed]
4. Barra, J.; Oujamaa, L.; Chauvineau, V.; Rougier, P.; Pérennou, D. Asymmetric standing posture after stroke is related to a biased egocentric coordinate system. *Neurology* **2009**, *72*, 1582–1587. [CrossRef]
5. Bonan, I.; Leman, M.; Legargasson, J.; Guichard, J.; Yelnik, A. Evolution of subjective visual vertical perturbation after stroke. *Neurorehabilit. Neural Repair* **2006**, *20*, 484–491. [CrossRef]
6. Piscicelli, C.; Perennou, D. Visual verticality perception after stroke: A systematic review of methodological approaches and suggestions for standardization. *Ann. Phys. Rehabil. Med.* **2017**, *60*, 208–216. [CrossRef]
7. Pérennou, D. Postural disorders and spatial neglect in stroke patients: A strong association. *Restor. Neurol. Neurosci.* **2006**, *24*, 319–334.
8. Baggio, J.A.; Mazin, S.S.; Alessio-Alves, F.F.; Barros, C.G.; Carneiro, A.A.; Leite, J.P.; Pontes-Neto, O.M.; Santos-Pontelli, T.E. Verticality perceptions associate with postural control and functionality in stroke patients. *PLoS ONE* **2016**, *11*, e0150754. [CrossRef]
9. Kheradmand, A.; Winnick, A. Perception of upright: Multisensory convergence and the role of temporo-parietal cortex. *Front. Neurol.* **2017**, *8*, 552. [CrossRef]
10. Rossi, S.; Hallett, M.; Rossini, P.M.; Pascual-Leone, A.; Safety of TMS Consensus Group. Safety, ethical considerations, and application guidelines for the use of transcranial magnetic stimulation in clinical practice and research. *Clin. Neurophysiol.* **2009**, *120*, 2008–2039. [CrossRef]
11. Santos-Pontelli, T.E.; Rimoli, B.P.; Favoretto, D.B.; Mazin, S.C.; Truong, D.Q.; Leite, J.P.; Pontes-Neto, O.M.; Babyar, S.R.; Reding, M.; Bikson, M.; et al. Polarity-dependent misperception of subjective visual vertical during and after transcranial direct current stimulation (tDCS). *PLoS ONE* **2016**, *11*, e0152331. [CrossRef] [PubMed]

12. Santos, T.E.; Favoretto, D.B.; Toostani, I.G.; Nascimento, D.C.; Rimoli, B.P.; Bergonzoni, E.; Lemos, T.W.; Truong, D.Q.; Delbem, A.C.; Makkiabadi, B.; et al. Manipulation of human verticality using high-definition transcranial direct current stimulation. *Front. Neurol.* **2018**, *9*, 825. [CrossRef] [PubMed]
13. Baier, B.; Suchan, J.; Karnath, H.O.; Dieterich, M. Neural correlates of disturbed perception of verticality. *Neurology* **2012**, *78*, 728–735. [CrossRef] [PubMed]
14. Nascimento, D.C.; Depetri, G.; Stefano, L.H.; Anacleto, O.; Leite, J.P.; Edwards, D.J.; Santos, T.E.; Louzada Neto, F. Entropy analysis of high-definition transcranial electric stimulation effects on eeg dynamics. *Brain Sci.* **2019**, *9*, 208. [CrossRef]
15. Vicente, R.; Wibral, M.; Lindner, M.; Pipa, G. Transfer entropy—A model-free measure of effective connectivity for the neurosciences. *J. Comput. Neurosci.* **2011**, *30*, 45–67. [CrossRef]
16. Pincus, S.M. Approximate entropy as a measure of system complexity. *Proc. Natl. Acad. Sci. USA* **1991**, *88*, 2297–2301. [CrossRef]
17. Richman, J.S.; Moorman, J.R. Physiological time-series analysis using approximate entropy and sample entropy. *Am. J. Physiol.-Heart Circ. Physiol.* **2000**, *278*, H2039–H2049. [CrossRef]
18. Fonteneau, C.; Mondino, M.; Arns, M.; Baeken, C.; Bikson, M.; Brunoni, A.R.; Burke, M.J.; Neuvonen, T.; Padberg, F.; Pascual-Leone, A.; et al. Sham tDCS: A hidden source of variability? Reflections for further blinded, controlled trials. *Brain Stimul.* **2019**, *12*, 668–673. [CrossRef]
19. Bossomaier, T.; Barnett, L.; Harré, M.; Lizier, J.T. Transfer entropy. In *An Introduction to Transfer Entropy*; Springer: Berlin/Heidelberg, Germany, 2016; pp. 65–95.
20. Aziz, N.A. Transfer entropy as a tool for inferring causality from observational studies in epidemiology. *bioRxiv* **2017**, 149625.
21. R Core Team. *R: A Language and Environment for Statistical Computing*; R Foundation for Statistical Computing: Vienna, Austria, 2019.
22. Mann, H.B.; Whitney, D.R. On a test of whether one of two random variables is stochastically larger than the other. *Ann. Math. Stat.* **1947**, *18*, 50–60. [CrossRef]
23. Wilcoxon, F. Individual Comparisons by Ranking Methods. *Biom. Bull.* **1945**, *1*, 80–83. [CrossRef]
24. Biabani, M.; Farrell, M.; Zoghi, M.; Egan, G.; Jaberzadeh, S. Crossover design in transcranial direct current stimulation studies on motor learning: Potential pitfalls and difficulties in interpretation of findings. *Rev. Neurosci.* **2018**, *29*, 463–473. [CrossRef] [PubMed]
25. Leshikar, E.D.; Leach, R.C.; McCurdy, M.P.; Trumbo, M.C.; Sklenar, A.M.; Frankenstein, A.N.; Matzen, L.E. Transcranial direct current stimulation of dorsolateral prefrontal cortex during encoding improves recall but not recognition memory. *Neuropsychologia* **2017**, *106*, 390–397. [CrossRef] [PubMed]
26. Long, J.A. Jtools: Analysis and Presentation of Social Scientific Data, 2020. R Package Version 2.1.0. Available online: https://cran.r-project.org/web/packages/jtools/index.html (accessed on 30 November 2021).
27. Genthon, N.; Rougier, P. Influence of an asymmetrical body weight distribution on the control of undisturbed upright stance. *J. Biomech.* **2005**, *38*, 2037–2049. [CrossRef] [PubMed]
28. Anker, L.C.; Weerdesteyn, V.; van Nes, I.J.; Nienhuis, B.; Straatman, H.; Geurts, A.C. The relation between postural stability and weight distribution in healthy subjects. *Gait Posture* **2008**, *27*, 471–477. [CrossRef] [PubMed]
29. Kamphuis, J.F.; de Kam, D.; Geurts, A.C.; Weerdesteyn, V. Is weight-bearing asymmetry associated with postural instability after stroke? A systematic review. *Stroke Res. Treat.* **2013**, *2013*, 692137. [CrossRef] [PubMed]
30. Marigold, D.S.; Eng, J.J.; Tokuno, C.D.; Donnelly, C.A. Contribution of muscle strength and integration of afferent input to postural instability in persons with stroke. *Neurorehabilt. Neural Repair* **2004**, *18*, 222–229. [CrossRef]
31. Marigold, D.S.; Eng, J.J. The relationship of asymmetric weight-bearing with postural sway and visual reliance in stroke. *Gait Posture* **2006**, *23*, 249–255. [CrossRef]
32. Mansfield, A.; Danells, C.J.; Inness, E.; Mochizuki, G.; McIlroy, W.E. Between-limb synchronization for control of standing balance in individuals with stroke. *Clin. Biomech.* **2011**, *26*, 312–317. [CrossRef]
33. Skarda, C.A.; Freeman, W.J. How brains make chaos in order to make sense of the world. *Behav. Brain Sci.* **1987**, *10*, 161–173. [CrossRef]
34. Huang, Y.; Holzel, R.; Pethig, R.; Wang, X.B. Differences in the AC electrodynamics of viable and non-viable yeast cells determined through combined dielectrophoresis and electrorotation studies. *Phys. Med. Biol.* **1992**, *37*, 1499–1517. [CrossRef] [PubMed]
35. Chialvo, D.R.; Gilmour, R.F., Jr.; Jalife, J. Low dimensional chaos in cardiac tissue. *Nature* **1990**, *343*, 653–657. [CrossRef] [PubMed]
36. Stein, K.M.; Walden, J.; Lippman, N.; Lerman, B.B. Ventricular response in atrial fibrillation: random or deterministic? *Am. J. Physiol.-Heart Circ. Physiol.* **1999**, *277*, H452–H458. [CrossRef] [PubMed]
37. Carroll, J.P.; Freedman, W. Nonstationary properties of postural sway. *J. Biomech.* **1993**, *26*, 409–416. [CrossRef]
38. Collins, J.J.; Luca, C.J.D. Open-loop and closed-loop control of posture: A random-walk analysis of center-of-pressure trajectories. *Exp. Brain Res.* **1993**, *95*, 308–318. [CrossRef]
39. Duarte, M.; Zatsiorsky, V.M. On the fractal properties of natural human standing. *Neurosci. Lett.* **2000**, *283*, 173–176. [CrossRef]
40. Gagey, P.M.; Martinerie, J.; Pezard, L.; Benaim, C. L'équilibre Statique Est Contrôlé par un Système Dynamique Non-Linéaire. 1998. Available online: http://ada-posturologie.fr/L'equilibrestatique1998.pdf (accessed on 28 February 2022).
41. Kerk, J.; Snyder, A.C.; Schot, P.K.; Myklebust, B.M.; Prieto, T.; Myklebust, J.; O'Hagan, K.P.; Clifford, P.S. The Effect of an Abdominal Binder on the Exercise Response of Paraplegic Wheelchair Athletes: 188. *Med. Sci. Sport. Exerc.* **1992**, *24*, S32. [CrossRef]

42. Oie, K.S.; Kiemel, T.; Jeka, J.J. Human multisensory fusion of vision and touch: Detecting non-linearity with small changes in the sensory environment. *Neurosci. Lett.* **2001**, *315*, 113–116. [CrossRef]
43. Fino, P.C.; Mojdehi, A.R.; Adjerid, K.; Habibi, M.; Lockhart, T.E.; Ross, S.D. Comparing Postural Stability Entropy Analyses to Differentiate Fallers and Non-fallers. *Ann. Biomed. Eng.* **2015**, *44*, 1636–1645. [CrossRef]
44. Donker, S.F.; Roerdink, M.; Greven, A.J.; Beek, P.J. Regularity of center-of-pressure trajectories depends on the amount of attention invested in postural control. *Exp. Brain Res.* **2007**, *181*, 1–11. [CrossRef]
45. Kędziorek, J.; Błażkiewicz, M. Nonlinear Measures to Evaluate Upright Postural Stability: A Systematic Review. *Entropy* **2020**, *22*, e22121357. [CrossRef] [PubMed]
46. Lipsitz, L.A. Dynamics of stability: The physiologic basis of functional health and frailty. *J. Gerontol. A Biol. Sci. Med. Sci.* **2002**, *57*, B115–B125. [CrossRef] [PubMed]
47. Lipsitz, L.A.; Goldberger, A.L.; Goldberger, A.L. Loss of 'complexity' and aging. Potential applications of fractals and chaos theory to senescence. *Jama* **1992**, *267*, 1806–1809. [CrossRef]
48. Busa, M.A.; van Emmerik, R.E.A. Multiscale entropy: A tool for understanding the complexity of postural control. *J. Sport Health Sci.* **2016**, *5*, 44–51. [CrossRef] [PubMed]
49. Louzada, F.; Nascimento, D.C.d.; Egbon, O.A. Spatial Statistical Models: An Overview under the Bayesian Approach. *Axioms* **2021**, *10*, 307. [CrossRef]
50. Paillard, T.; Noé, F. Techniques and methods for testing the postural function in healthy and pathological subjects. *BioMed Res. Int.* **2015**, *2015*, 891390. [CrossRef] [PubMed]
51. Bürkner, P.C. brms: An R package for Bayesian multilevel models using Stan. *J. Stat. Softw.* **2017**, *80*, 1–28. [CrossRef]
52. R Core Team. *R: A Language and Environment for Statistical Computing*; R Foundation for Statistical Computing: Vienna, Austria, 2021.
53. Team, S.D. Stan modeling language users guide and reference manual. Version 2.12 *Tech. Rep.* **2016**.